



HYBRID METHOD FOR DETERMINATION OF POWER SYSTEMS DYNAMIC EQUIVALENTS BASED ON MEASUREMENTS

OMAR BENMILOUD, SALEM ARIF

Key words: Dynamic equivalents, Model order reduction, Measurement-based approach, Transient stability, Cuckoo search (CS) algorithm, Chaotic salp swarm algorithm (CSSA).

Dynamic equivalence is an important process of electrical power systems. It allows performing transient stability assessment of a specific area at a minimum cost. In this paper, the fourth-order model of synchronous generators with a simple exciter is used as an equivalent to the group of generators in the external area. Based on the post fault measurements, parameters of the equivalent are estimated by an optimal procedure. In this procedure, a Low-Level Teamwork Hybrid (LTH) algorithm based on Cuckoo search (CS) and the Chaotic Salp Swarm Algorithm (CSSA) is employed. The developed program is tested on two standard power systems used by most authors who have dealt with this problem. Simulation results confirm the ability of the reduced model to preserve the main dynamics of the original system with accuracy. A comparative study of the LTH approach against recently proposed metaheuristics proved the superiority of the proposed algorithm.

1. INTRODUCTION

With the accelerating growth of the power systems in the form of regional interconnections and the new diverse transmission structure driven by the competitive market, safe and stable operations of the system have become critical. Transient Stability Assessment (TSA) based on numerical integration methods or the Step-By-Step (SBS) in time-domain is considered the most reliable and accurate method in which the Differential-Algebraic Equations (DAEs) are solved. However, performing such analysis on large-scale systems can be costly and time-consuming. In this regard, if the whole system is being replaced by an equivalent that maintains its dynamic characteristics, the simulation time of TSAs is expected to decline significantly [1–3].

The concept of Dynamic Equivalence (DE) was introduced in the middle of the last century. The problem has been investigated extensively by power system researchers and remains one of the most popular topics due to the challenges it poses. DE programs aim simply to reduce the overwhelmed of presenting large systems by replacing portion of the system with an equivalent [4], this portion is often a large system with certain electrical distant or geographical extent referred to as External Subsystem (ES), the remainder parts represents the Internal Subsystem (IS), this subsystem is the primary focus of the study, therefore it must be retained in detail. A good equivalent model should reproduce with accuracy the steady-state and the dynamic characteristics of the original system including the external system, while at the same time being compatible with the available simulation packages for power system analysis.

Typically, the dynamic equivalent methods include two approaches classified as [5]: (i) reduction-based approaches [6–10]; and (ii) measurement-based approaches [11–18]. The former is based on the aggregation/elimination of the ESs with the assumption that information on the structures and parameters of the whole system are available. However, in reality, such systems may be owned by different utilities. Thus, information of the ES is not necessarily accessible. Whereas the latter focused on the power system measured response collected within the IS

determined either from real-time measurements or from simulation programs [19]. This way, the major drawback of the reduction-based approaches is overcome.

Dynamic equivalent based on measurements could play a vital role regardless of the unknown configuration and parameters of the external systems. The main procedure in DE measurement-based methods consists of determining optimum settings of control variables such as: parameters of the equivalent generators, gain and time constants of the equivalent voltage regulators, etc. Following which, the dynamics of the reduced system become identical to those in the original system when subjected to the same disturbance. This can be achieved by the fulfillment of certain objective functions. In the search of optimal settings, the equivalent must satisfy constraints on variables' feasibility and steady-state conditions.

In the early days [20, 21], the usual formulation of DE involved traditional search algorithms to find parameters of the equivalent, these algorithms are usually sensitive to the initial condition, therefore, there is a big chance the algorithm diverges or gets stuck in a local optimum if the initial point is not close enough to the global solution. Recently, a large number of metaheuristic optimization have been utilized to deal with this issue. Among them, the following techniques are highlighted and discussed in [11, 12, 22–24]: (i) Multi-objective Salp Swarm Algorithm (MSSA); (ii) Mean-Variance Mapping Optimization (MVMO) with multi-parent crossover; (iii) Modified Genetic Algorithms (MGA) with a selected initial population; (iv) Genetic Algorithm and the Grey-Box approach (GA-GB); and (v) Grey Wolf Optimizer (GWO).

Due to the complex nature of the power system dynamics, these algorithms may still occasionally be trapped into some local optima. In fact, there is room for improvement. An algorithm that combines the merits of global and local search algorithms is needed. This paper proposed a hybrid model based on the Cuckoo Search algorithm (CS). In this model, the Chaotic Salp Swarm Algorithm (CSSA) is embedded in cascade with CS to tune the best solution found after each iteration of CS. The goal of the incorporation is to enhance the local search by exploiting the most promising regions located by CS. In the

hybrid model, CS serves as a global search algorithm through the large steps provided by the well-known Lévy flight model. This way, it is expected that the accuracy of the equivalent model will be improved and a more precise model can be attained.

Moreover, it goes without saying that the identified parameters depend on the disturbance used to set the transient behavior, which makes these parameters only valid to those disturbances with a similar impact. Under such conditions, the reduced system and the original one may not be consistent dynamically anymore. In fact, there is room for improvement here too. For example with regard to the parameter dependence, utilizing extra scenarios (disturbances) with different impacts on the system should prevent the dependence of the model's parameters on a particular event.

The remaining part of the paper proceeds as follows: section 2 outlines the problem formulation. Section 3 gives a brief review of CS and CSSA and presents the details of the proposed hybrid approach. Application of the proposed is presented in section 4. Finally, section 5 summarizes the principal findings and draws conclusions.

2. EQUIVALENT MODEL STRUCTURE

In this paper, the adopted approach is to remove all buses in the external system except the border buses, that is, those buses in the internal system linked directly to the external areas. At such buses, equivalents are placed to resemble the dynamics of the target external areas [25].

2.1. MACHINE MODEL

Dynamics of the external areas are represented by virtual generators, which can be of any order [1]. In this paper, the fourth-order model of synchronous generators describing the transient dynamics on the d and q axes is used for simplicity. A common description is given as:

$$\begin{aligned} \frac{d\delta}{dt} &= \Omega_b(\omega - 1) \\ \frac{d\omega}{dt} &= \frac{1}{2H} (P_m - P_e - r_a I^2 - D(\omega - 1)) \\ \frac{dE'_q}{dt} &= \frac{1}{T'_{d0}} \left(-f_s(E'_q) - i_d(x_d - x'_d) \right) \\ \frac{dE'_d}{dt} &= \frac{1}{T'_{q0}} \left(-E'_d + i_q(x_q - x'_q) \right) \end{aligned} \quad (1)$$

where δ (rad/s), ω (pu) and Ω_b are the rotor angular position, speed, and base frequency. P_m (pu) and P_e (pu) are the mechanical input power and the electrical output power, respectively. E'_d (pu) and E'_q (pu) are the transient voltages along the d -axis/ q -axis. x_d (pu), x_q (pu), x'_d (pu) and x'_q (pu) are the steady-state and transient reactances along the d -axis/ q -axis, respectively. T'_{d0} (s), T'_{q0} (s) are the open transient circuit time constants along the d -axis/ q -axis. r_a (pu), H (s) and D (pu) are the armature resistance, acceleration time constant and damping coefficient, respectively. i_d and i_q are the currents along the d -axis/ q -axis and f_s is the magnetic saturation function. In the time domain simulations, the Power System Toolbox (PST) verifies that the transient reactances along the d -axis and q -axis are equal, in such case where $x'_d \neq x'_q$, PST set the

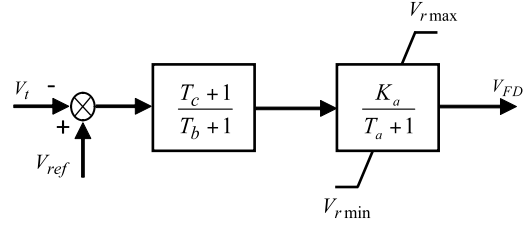


Fig. 1 – Block diagram of the equivalent exciter.

value of the quadrature reactance as $x'_q = x'_d$. This reduces the total number of parameters to be estimated for the virtual generator to 8 parameters given as:

$$\mathbf{\alpha}_{gen} = \{r_a, x_d, x_q, x'_d, T'_{d0}, T'_{q0}, H, D\}. \quad (2)$$

2.2. AUTOMATIC VOLTAGE REGULATOR

In this paper, the generator is equipped with a simple exciter which is defined as the primary voltage regulator. Based on the exciter block diagram shown in Fig. 1, the parameters that need to be estimated for the excitation system are given as:

$$\mathbf{\alpha}_{exc} = \{K_a, T_a, T_b, T_c\}. \quad (3)$$

Where K_a (pu) is the voltage regulator gain constant. T_a (s), T_b (s) and T_c (s) are the time constants for the voltage regulator and the transient gain reductions, respectively. V_{min} (pu) and V_{max} (pu) are the minimum and the maximum voltage regulator outputs, respectively.

Notice that, the 4th order model of synchronous generators with a simple exciter is used as an equivalent to the group of generators in the ES. From the equations above, it can be seen that there is a total of 12 parameters to be estimated. The overall decision variables for the i^{th} equivalent model are given as: $\mathbf{\alpha} = \{r_a, x_d, x_q, x'_d, T'_{d0}, T'_{q0}, H, D, K_a, T_a, T_b, T_c\}$. These parameters are to be estimated using the optimal approach that will be explained section 3.

2.3. STEADY STATE PRESERVATION

As illustrated in Fig. 2, the steady-state operating conditions must be preserved. This can be done using a load flow study, where the complex power injected by the virtual generators at border buses can be calculated. Hence, the nodal balance equation for the i^{th} border bus yields [25].

$$\sum_{k \in K} P_{ik} + P_{Gi} + P_{Li} = 0. \quad (4)$$

where K is the set of nodes connected directly to the i^{th} border bus, P_{ik} is the active power flow through the transmission line connecting buses i and k . P_{Gi} and P_{Li} are the produced and consumed powers at the i^{th} border bus, respectively. The voltage at each border bus is set to the value calculated in the unreduced system. Therefore, the complex power flows from the original and equivalent system are precisely matched.

2.4. PARAMETERS IDENTIFICATION

The aim of a dynamic equivalent program is to reduce the complexity of external areas by reducing the amount of DAEs that govern the model's dynamic behavior. After the reduction, the responses of the reduced system must fit the original system responses when disturbances (i.e.,

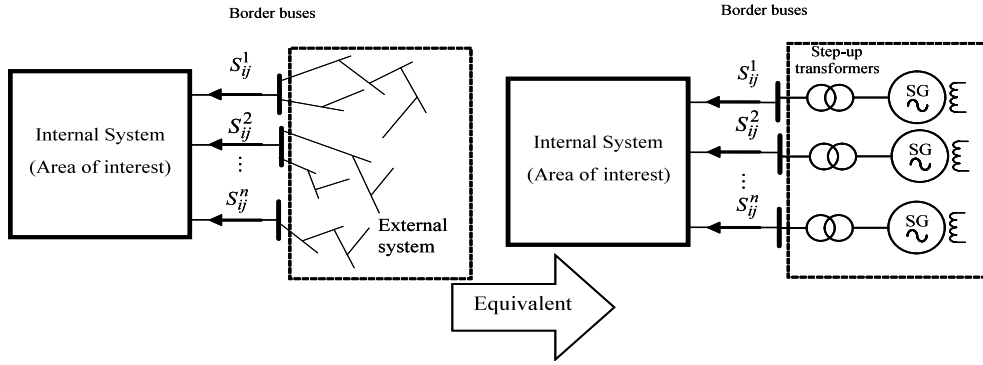


Fig. 2 – Dynamic equivalent model structure: From the detailed to the simplified.

perturbation of any kind) take place in the internal system. Using the original system responses as a reference, parameters of the equivalent are identified by comparing the reference signals with the same signals obtained from the time domain simulations in the reduced system. In this paper, active and reactive power responses of those generators in the internal system are set as reference signals. Mathematically, the objective function by which the optimal set of parameters \mathbf{a}^* are obtained is formulated as follows:

$$\min F(\mathbf{a}) = \min (\varepsilon_P(\mathbf{a}) + \varepsilon_Q(\mathbf{a})), \quad (5)$$

$$\left\{ \begin{array}{l} \varepsilon_P(\mathbf{a}) = \sum_{j=1}^{np} \rho_j \sum_{i=1}^{N_G} \left(\sum_{k=1}^{N_K} (P_{G_i}^{orig}(t_k) - P_{G_i}^{red}(\mathbf{a}, t_k)) \right) \\ \varepsilon_Q(\mathbf{a}) = \sum_{j=1}^{np} \rho_j \sum_{i=1}^{N_G} \left(\sum_{k=1}^{N_K} (Q_{G_i}^{orig}(t_k) - Q_{G_i}^{red}(\mathbf{a}, t_k)) \right) \end{array} \right\}, \quad (6)$$

where P_G^{orig} and Q_G^{orig} are the active and reactive powers of the internal system generators in the original system at different instants. P_G^{red} and Q_G^{red} are the same variables obtain from the reduced system in the same instants. N_K , N_G and np are the total number of time samples for the transient, the total number of generators in the study system and the total number of disturbances, respectively. t_k is the k^{th} time sample. ρ_j is the weighting factor of the j^{th} disturbance. In this study, $\rho_j = 1/np$ for all disturbances. The objective function in (5) is subjected to the side constraint:

$$\alpha_i^{\min} \leq \alpha_i \leq \alpha_i^{\max}, \quad (7)$$

where α_i^{\min} and α_i^{\max} are the minimum and maximum values of the i^{th} parameter selected based on the values provided in [27].

Identification of the adequate vector parameters \mathbf{a}^* is particularly valuable when attempting to build an equivalent to the external system. However, due to the non-convex landscape and non-linearity of the power system dynamics, the parameter identification in (5) appears to be a complex multimodal optimization problem that requires a robust optimization technique. In this regard, the next section presents the details of the proposed hybrid algorithm used to carry the identification.

3. BRIEF OVERVIEW OF CS AND CSSA ALGORITHMS

Metaheuristic algorithms have been used extremely by many researchers in the field of optimization due to their

ability to escape the local minima [28,29]. These algorithms are considered global optimization techniques that use a trade-off between exploitation and exploration in order to ensure that the global optimality is achievable [30]. Nevertheless, these algorithms have their own drawbacks. Therefore, hybridization of different metaheuristics received considerable interest as it combines the merits of at least two algorithms to improve the overall search efficiency [31,32]. In this section, the two-parent algorithms CS and CSSA are introduced to set up the appropriate background for the hybrid method.

3.1. CUCKOO SEARCH ALGORITHM (CS)

The Cuckoo Search (CS) is a population-based algorithm inspired by the strange behavior of some cuckoo species. It is a metaheuristic search algorithm that generally explores the search space using the Lévy step [33, 34]. Cuckoo birds have a peculiar reproduction strategy that involves the female laying her fertilized eggs in the nest of other species so that a suitable host will unwittingly raise her offspring. As a consequence, if the host bird discovers the alien eggs he will either throw the eggs away or simply abandon the nest and build a new one elsewhere. Iteratively, replacement of the nest may lead to improve the quality of the solution over time, achieving finally a very good solution for the studied problem.

In order to get the simplest model of the CS algorithm, the following idealized rules are developed:

1. Each cuckoo lays one egg once at a time and allows it to incubate in a randomly chosen nest.
2. The nests with high quality of eggs (*i.e.*, solutions) are maintained until the next generation.
3. The number of available bird nests n is fixed, and the possibility of discovering a deposited egg by the nest's owner is denoted by $p_a \in [0, 1]$.

Based on the hypotheses above, and in an environment of n cuckoos, the nest seeking behavior of i^{th} cuckoo obeys the Lévy flight model. The path and the location are updated using the formula below:

$$Pos_i^{t+1} = Pos_i^t + \beta \oplus Lévy(\gamma) \quad \text{for } i = 1, 2, \dots, n. \quad (8)$$

Where Pos_i^{t+1} and Pos_i^t represent the new and current locations of the i^{th} nest, respectively. $\beta > 0$ is the step size constant, whose value is usually taken equal to 0.01 [33]. $Lévy(\gamma)$ is a random walk through the Lévy flight model [35]. And point-to-point multiplication is denoted by \oplus .

The Lévy flight in (8) denotes the global explorative random walk in which the next location only depends on the current location. The steps are defined in terms of the

step-lengths, which have a certain probability distribution (i.e., the Lévy distribution given in (9)).

$$Lévy \sim \mu = t^{-\gamma}, \quad (1 \leq \gamma \leq 3). \quad (9)$$

This has an infinite mean with infinite variance. Now, the consecutive jumps/steps of cuckoos basically form a random walk procedure which obeys a power-law step-length distribution with a heavy tail. Pseudo code of the Cuckoo Search (CS) algorithm is granted in Fig. 3.

Set the host nest size n , the discovering probability p_a and the maximum number of generation Max_{itr} .

```

for  $i=1:n$  do
  Initialize randomly population of  $n$  host  $Pos_i^t$ 
  Evaluate the fitness of each nest  $f(Pos_i^t)$ 
end for
While  $t < Max_{itr}$  do
  Generate new solutions (cuckoos)  $Pos_i^{t+1}$  randomly via Lévy flight using (8)
  Evaluate the fitness of the solutions  $f(Pos_i^{t+1})$ 
  Pick randomly a nest  $Pos_j$ , among  $n$  solutions
  if  $f(Pos_i) < f(Pos_j)$  then
    Replace the solution  $Pos_j$  by the solution  $Pos_i$ 
  end if
  Abandon a portion  $p_a$  of worse nests and build new ones at new locations using Lévy flight
  Keep the best solutions (nests with quality solutions)
  Sort the solution and find the current best
  Set  $t=t+1$ . {Iteration counter increasing}
end while
Save the best solution as the optimal solution.

```

Fig. 3 – Pseudo code of the CS algorithm.

3.2. CHAOTIC SALP SWARM ALGORITHM (CSSA)

The sea salp is a barrel-shaped, transparent tunicate that moves by the act of jet propulsion. To initiate movement, sea salps create unidirectional water flow by taking water at one end and expelling it at the other end. In the ocean, these gelatinous oddities usually travel in colonies in the form of large chains called “salp chains”. The swarm includes one leader whose primary role is to guide the swarm to the best location of food by searching the most promising regions. For this reason, the leader is located at the head of the chain. The remainder salps are followers, and as their name indicated their role is to follow each other and their leader. Inspired by the swarming mechanism, Mirjalili et al. in 2017 proposed a novel optimization algorithm under the name of Salp Swarm Algorithm (SSA) [36].

Given the environment of n salps, and based on the food-seeking behavior, the i^{th} salp updates its position using the formulas below:

1. The leader salp changes position with respect to the food source as:

$$Pos_j^1 = \begin{cases} Food_j + r_1 \left(r_2 (ub_j - lb_j) + lb_j \right) & r_3 < 0.5 \\ Food_j - r_1 \left(r_2 (ub_j - lb_j) + lb_j \right) & r_3 \geq 0.5 \end{cases} \quad (10)$$

Where Pos_j^1 and $Food_j$ are the position of the leader salp and its target food source in the j^{th} dimension; lb_j and ub_j are the lower bound and the upper bound in the j^{th} dimension, respectively. r_2 and r_3 are two numbers

randomly generated in the interval $[0,1]$.

The coefficient r_1 is viewed as the main controlling parameter of SSA because it maintains equilibrium between exploration and exploitation. The coefficient r_1 is calculated as:

$$r_1 = 2e^{-\left(\frac{4t}{Max_{itr}}\right)^2} \quad (11)$$

2. The follower salps change position based on Newton’s law of motion as:

$$Pos_j^i = \frac{1}{2} at^2 + v_0 t \quad (12)$$

where $i \geq 2$, Pos_j^i is the position in the j^{th} dimension of the i^{th} follower salp, and v_0 is the initial speed taken as 0. t is time (in optimization giving by an iteration), therefore, $\Delta t = 1$.

From the assumptions above, the eq. (12) that governs the followers’ movements can be simplified to:

$$Pos_j^i = \frac{Pos_j^i + Pos_j^{i-1}}{2} \quad (13)$$

In [37] it was demonstrated that employing chaotic maps to replace random variables in the original SSA, performances of the algorithm have improved. In this paper, and similar to the modification introduced in [37], r_2 is updated using the logistic chaotic map with the initial value of 0.7. The pseudo code of the Chaotic Salp Swarm Algorithm (CSSA) is granted in Fig. 4.

Set the number of salps n , the maximum number of generation Max_{itr} , and the search boundary vectors ub and lb .

Initialize randomly population of n salps Pos

Evaluate the fitness of each salp $f(Pos^i)$

Update the leader salp $Food = \min(Pos^i)$

While $t < Max_{itr}$ **do**

Update r_1 using (11), and r_2 using the logistic map

for $i=1:n$ **do**

if ($i=1$) **then**

Update the position of the leader salp using (10)

else

Update the position of the follower salp using (13)

end if

end for

Update the leader salp $Food = \min(Pos^i)$

Set $t=t+1$. {Iteration counter increasing}

end while.

Fig. 4 – Pseudo code of the CSSA algorithm.

3.3. HYBRID APPROACH

CS is a recent population-based algorithm that shows superior results in many optimization problems. The original algorithm explores the search space using large steps via Lévy flight. These long-distance movements help search agents (cuckoos) to escape from the local optimum. Such merits clearly indicate that CS has good global exploration capabilities. Meanwhile, CSSA has good local exploitation capabilities using the control parameter coefficient r_1 and the dependent movements of followers on

each other. Combining the merits of the aforementioned algorithms, this paper proposes a Low-Level Teamwork Hybrid (LTH) based on CS and CSSA algorithms. In LTH, CSSA algorithm is embedded in cascade with CS to tune the best solution found after each iteration of CS. This approach is named CS-CSSA. In which the goal of CSSA is to enhance the local search by exploiting the most promising regions after a full iteration of CS. Pseudo code of CS-CSSA is provided in Fig. 5.

- Step 1:** Define the control parameters of CS and CSSA.
Step 2: Initialize randomly population of n agent.
Step 3: Execute one iteration of CS.
Step 4: Execute one iteration of CSSA to fine-tune the results obtained by CS.
Step 5: Repeat steps 3–4 until the stop criteria are satisfied.
Step 6: Save the final solution as the optimal solution.

Fig. 5 – Pseudo code of the CS-CSSA algorithm.

4. SIMULATION RESULTS

All of the following experiments were completed on Lenovo ThinkPad T470 personal computer, running on Intel® Core™ i7-7500U CPU, 2.70 GHz processing speed, and installed memory (RAM) of 8 GB. The main procedure of the proposed algorithm is to generate candidate parameters to the equivalent model. Using these potential parameters, transient stability studies are carried out for all disturbances using PST toolbox to evaluate the objective function in (5). These steps are iteratively repeated until the maximum number of generations is exceeded. It is worthwhile to mention that CS and CSSA equally shared the total number of iterations.

To validate the developed program, two standard power systems used by most authors who have dealt with this problem were tested. The tested networks are the 39-bus system commonly known as the New England (NE) and the 68-bus system commonly known as the Northeast Power Coordinating Council (NPCC).

4.1. TEST SYSTEM

The NE system in Fig. .6 consists of 10 generators, 46

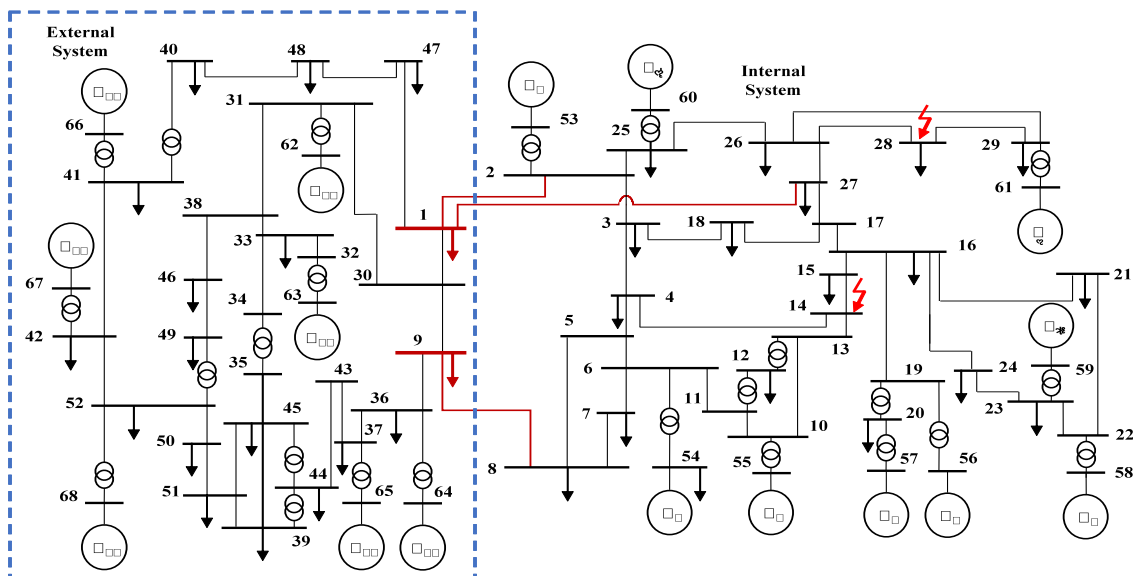


Fig. 7 – Northeast power coordinating council system.

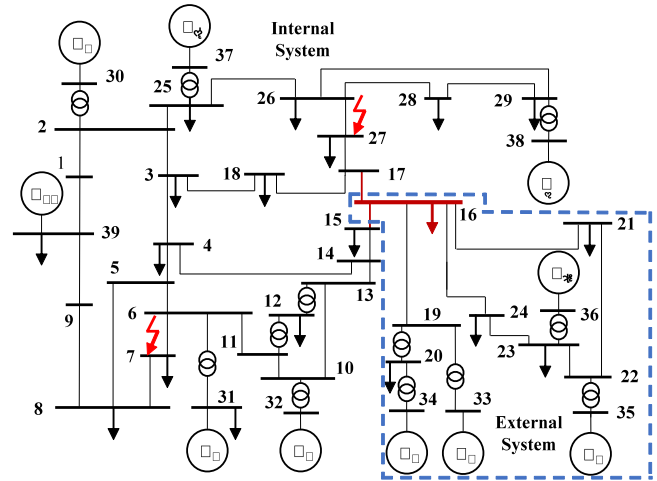


Fig. 6 – New England system.

transmission lines, and 12 transformers with a total capacity of ($P_{G-total} = 6.19$ GW, $Q_{G-total} = 2.28$ GVar). The area in the blue square represents the system to be reduced, while the rest is the system of interest. As can be seen, the equivalent generator should be placed at the border bus (i.e., bus 16) and linked to the study area through the two tie lines 16-15 and 16-17. Two disturbances (three-phase faults) at different locations in the internal system are used (i.e., bus 7 and bus 27), each disturbance is provoked at $t=0$ and lasts 6 cycles before the protection disconnects the associated transmission line to eliminate the fault. For each scenario, system responses are observed in a closed interval of 3 seconds.

The NPCC system in Fig. 7 consists of 16 generators, 86 transmission lines, and 20 transformers with an installed capacity of ($P_{G-total} = 18.408$ GW, $Q_{G-total} = 2.79$ GVar). The area in the blue square represents the system to be reduced, while the rest is the system of interest. As can be seen, there should be two equivalent generators placed at border buses, those are, bus 1 and bus 9, respectively. The equivalents are linked to the study area through the transmission lines 1-2, 1-27 and 9-8. Two disturbances (three-phase faults) at different locations in the internal system are used (i.e., bus 14 and bus 28), each disturbance is triggered at $t = 0$ and lasts 6 cycles before the protection

removes the associated transmission line to eliminate the fault. For each scenario, system responses are observed in a closed interval of 3 seconds.

4.2. RESULTS AND DISCUSSION

Like any metaheuristic algorithm, it is essential to determine adequate control parameter values whose choice often depends on the studied problem. In this paper, and after several preliminary tests, the control parameters of the proposed CS-CSSA algorithm were set as given in Table 1. In order to obtain the most representative results, the estimated values of the equivalent models granted in Table 2 are the average result computed from 30 independent runs.

Table 1
CS-CSSA Control Parameters

Parameters	39-bus	68-bus
Number of Cuckoos/Salps	20/20	25/25
Maximum iteration (CS/CSSA)	50/50	50/50
Discovery Rate	0.275	0.275

Table 2
Estimated parameters for the equivalent generator

Parameters	68-bus		
	G _{eq1}	G _{eq2}	G _{eq3}
r_a	0.0022	0.0037	0.0050
x_d	2.0880	1.3764	2.2925
x_q	2.2549	1.0017	1.0000
x'_d	0.3597	0.1501	0.1513
T'_{d0}	4.2573	7.1597	3.6060
T'_{q0}	1.5538	2.0000	1.9921
H	13.7683	334.8433	62.3755
D	1.1733	1.0466	0.7680
K_a	31.7567	12.0109	127.4033
T_a	0.4640	5.91e-07	6.68e-07
T_b	0.3286	0.0400	13.4820
T_c	0	0.8725	1.4747

To confirm the ability of the reduced model to preserve the main dynamic responses of the original system, different scenarios (i.e., three-phase faults) differ from those applied for the estimation were used. Then, transient responses are observed for 10 seconds once using the original system and once using the reduced system including the optimized equivalents. The goal is to demonstrate that the reduced system responses are consistent with those measured from the unreduced system.

For this reason, the formula in eq. (14) is employed to compare the main signals:

$$Error = \sqrt{\frac{1}{N} \sum_{k=1}^N \left(Y_i^{orig}(t_k) - Y_i^{red}(t_k) \right)^2}, \quad (14)$$

where Y_i^{orig} and Y_i^{red} are the same signals measured from the original system and equivalent system, respectively when both systems are subjected to the same disturbance. t_k is the k^{th} sample in time, and N denotes the number of samples. The criteria in (14) is used to evaluate the performance of the equivalent. That is, how well the equivalent fits the original system dynamically. Using (14), Tables 3 and 4 summarize the accuracy evaluation for the two systems under different faults.

For the 39-bus system, Table 3 summarizes the accuracy evaluation for the six generators in the internal system following three-phase faults near buses 3, 8, 10 and 14,

respectively. The largest error is obtained for the fault at bus 3; this error is mainly contributed by generator 10. This is due to the fact that generator 10 has the largest power output. However, the average value for the fault at bus 3 indicates that the equivalent generator is able to predict the dynamics of the original system even for disturbances different from those used in the estimation.

Table 3
Accuracy evaluation of the (NE) system

Fault location		Bus 3	Bus 8	Bus 10	Bus 14
P_e	Max Error	2.0212	1.1382	1.3291	1.6417
	Avg Error	0.3514	0.2250	0.3425	0.3067
Q_e	Max Error	0.5454	0.3934	0.3313	0.4525
	Avg Error	0.2113	0.1593	0.1351	0.1832

Table 4
Accuracy evaluation of the (NPCC) system

Fault location		Bus 3	Bus 13	Bus 16	Bus 27
P_e	Max Error	0.0533	0.0588	0.0858	0.0519
	Avg Error	0.0425	0.0384	0.0569	0.0402
Q_e	Max Error	0.0361	0.0265	0.0412	0.0347
	Avg Error	0.0237	0.0201	0.0335	0.0229

For the 68-bus system, the overall accuracy measurement results for the nine generators in the internal system following three-phase fault near buses 3, 13, 16 and 27 are presented in Table 4. In this system, the largest error is obtained for the fault at bus 16.

Figures 10 and 11 report time-domain responses of the dynamic equivalent and the original system for some representative signals under three-phase faults. Evaluation of the resulting plots for the NE system in Fig. 10 illustrates that the overall tendency of the generators in the internal system is preserved. By analyzing Fig. 11, we can clearly see that the estimated equivalent is able to maintain the original system behavior also for faults different from the scenarios used in the estimation phase.

4.3. COMPARATIVE STUDY

In this section, the proposed CS-CSSA algorithm will be checked from different aspects on the 39 and 68 test systems. Likewise, the algorithm will be compared to other metaheuristics in terms of average and best solution values obtained by minimizing the objective function. In order to have a fair comparison among the algorithms, all executions are performed under the same conditions (i.e. the same number of populations, iterations and the same boundary limits). The results reported below are computed over thirty independent runs. The corresponding control parameters of the CS-CSSA are defined according to Table 1.

The average execution time of the original CS is 8040 s for the 39-bus and 17031 s for the 68-bus system. On the other hand, the proposed algorithm tremendously reduces the computation efforts with an average execution time of 5728 s and 9948 s, respectively. This is a time reduction of 28.75 % and 41.58 %, respectively.

Moreover, the optimization is performed by comparing the CS-CSSA approach against other metaheuristic algorithms. The selected algorithms for the comparative study are the original Cuckoo Search (CS) [33], Salp Swarm Algorithm (SSA) [37], Sine Cosine Algorithm (SCA) [38] and Harris Hawks Optimization (HHO) [39]. These

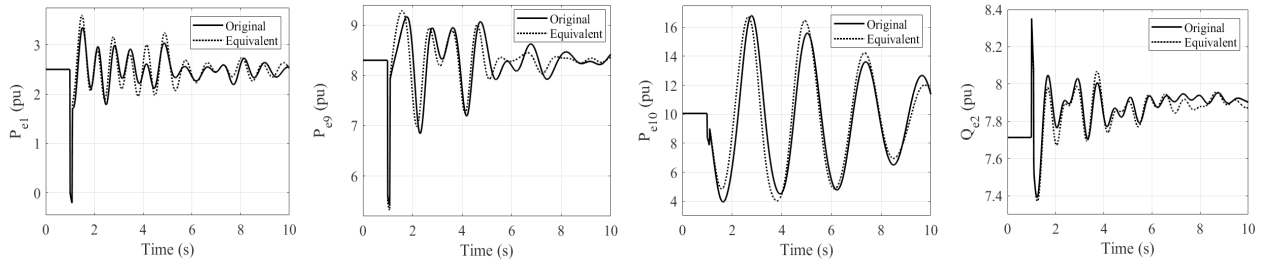


Fig. 10 – Transient stability simulations of the 39-bus system (Left to right, P_{e1} for fault at bus 3, P_{e9} for fault at bus 14, P_{e10} and Q_{e2} for fault at bus 8).

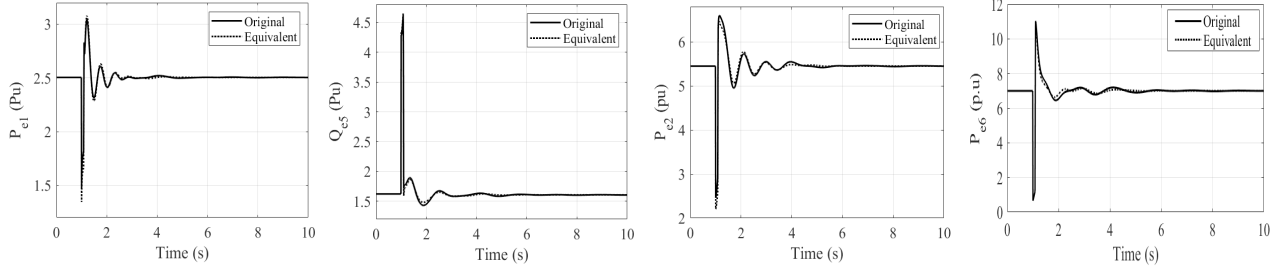


Fig. 11 – Transient stability simulations of the 68-bus system (Left to right, P_{e1} and Q_{e5} for fault at bus 13, P_{e2} for fault at bus 3 and P_{e6} for fault at bus 16).

metaheuristic algorithms have shown excellent performance when applied to various types of problems, including power system applications. Therefore, they would serve as a good reference to evaluate the capability of the proposed algorithm.

The convergence characteristics showing the objective function versus the number of iterations for the compared algorithms are plotted in Fig. 12 and Fig. 13. As can be seen, the proposed algorithm exhibits a better convergence compared to other metaheuristics. This is due to the incorporation of CSSA in the original algorithm. After each execution of CS, the search process is shifted to the fine tuning to speed up the convergence for the global optimum. Therefore, the CS-CSSA finds an optimum more accurately and precisely.

5. CONCLUSIONS

Dynamic equivalents based on measurement could play a vital role regardless of the unknown configuration and parameters of the external systems. In this paper, using only the post fault measurement, parameters of the equivalent were estimated by an optimal procedure.

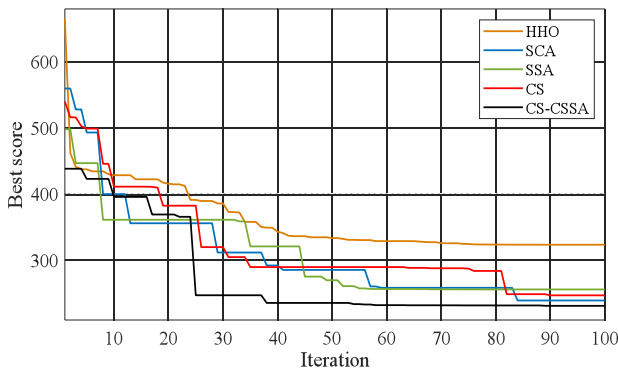


Fig. 12 – Convergence characteristics of the 39-bus system obtained by different algorithms.

A hybrid algorithm based on cuckoo search and the chaotic salp swarm algorithm was proposed. Simulation results were carried on 39-bus and 68 bus systems and the ability of the proposed hybrid algorithm to estimate parameters to the equivalent was confirmed through

accuracy tests. Moreover, evaluation of the time domain plots proved that the equivalent generator is able to predict the dynamics of the original system even for disturbances different from the ones used in the estimation. A comparative study of the CS-CSSA approach against recently proposed metaheuristics proved the superiority of the proposed algorithm.

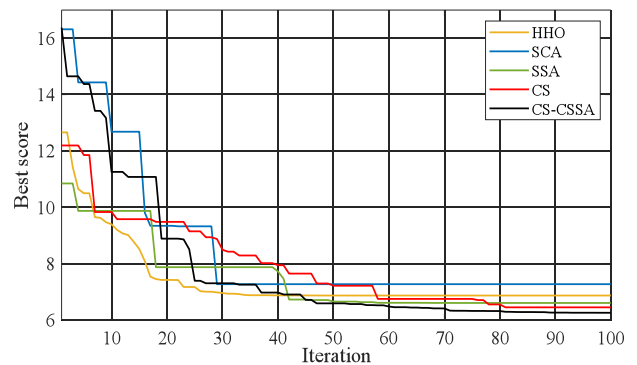


Fig. 13 – Convergence characteristics of the 68-bus system obtained by different algorithms.

Received on August 31, 2019

REFERENCES

1. P. Ju, L. Q. Ni, F. Wu, *Dynamic equivalents of power systems with online measurements. Part 1: Theory*, IEE Proc.-Gener. Transm. Distrib., **151**, 2, pp. 175–178 (2004).
2. P. Kundur, J. Paserba, V. Ajjarapu, G. Andersson, A. Bose, C. Canizares, N. Hatziargyriou, D. Hill, A. Stankovic, C. Taylor, T. Van Cutsem, V. Vittal, *Definition and Classification of Power System Stability*, IEEE Trans. on Power Syst., **19**, 3, pp. 1387–1401 (2004).
3. D. Osipov, K. Sun, *Adaptive nonlinear model reduction for fast power system simulation*, IEEE Trans. on Power Syst., **33**, 6, pp. 6746–6754 (2018).
4. R. Podmore, *Identification of coherent generators for dynamic equivalents*, IEEE Trans. on Power Appar. and Syst., **PAS-97**, 4, pp. 1344–1354 (1978).
5. R. Singh, M. Elizondo, S. Lu, *A review of dynamic generator reduction methods for transient stability studies*, IEEE Power and Energy Society General Meeting, San Diego, CA, USA, 2011.

6. A. M. Miah, *Study of a coherency-based simple dynamic equivalent for transient stability assessment*, IET Gener., Transm. & Distrib., **5**, 4, pp. 405–416 (2011).
7. B. Marinescu, B. Mallem, L. Rouco, *Large-scale power system dynamic equivalents based on standard and border synchrony*, IEEE Trans. on Power Syst., **25**, 4, pp. 1873–1882 (2010).
8. J. H. Chow, *Power System Coherency and Model Reduction*, USA: Springer, New York, 2013, pp. 39–72.
9. J. L. Jardim, A. M. L. Da Silva, *A methodology for computing robust dynamic equivalents of large power systems*, Electric Power Systems Research, **143**, pp. 513–521 (2017).
10. J. H. Chow, R. Galarza, P. Accari, W. W. Price, *Inertial and slow coherency aggregation algorithms for power system dynamic model reduction*, IEEE Trans. on Power Syst., **10**, 2, pp. 680–685 (1995).
11. R. Gueddouche, M. Boudour, *Intelligent non-linear dynamic equivalent approach applied to Algerian power system*, IET Gener., Transm. & Distrib., **13**, 14, pp. 2919–2929 (2019).
12. J. L. Rueda, J. Cepeda, I. Erlich, D. Echeverría, G. Argüello, *Heuristic optimization-based approach for identification of power system dynamic equivalents*, Int. J. of Electrical Power & Energy Syst., **64**, pp. 185–193 (2015).
13. A. T. Sarić, M. T. Transtrum, A. M. Stanković, *Data-driven dynamic equivalents for power system areas from boundary measurements*, IEEE Trans. on Power Syst., **34**, 1, pp. 360–370 (2019).
14. J. M. Ramirez, G. G. Garcia, *Model order reduction by a statistical metric*, IEEE PES Innovative Smart Grid Technologies Conference - Latin America (ISGT Latin America), Quito, Ecuador, 2017.
15. M. R. A. Paternina, J. M. Ramirez-Arredondo, J. D. Lara-Jiménez, A. Zamora-Mendez, *Dynamic equivalents by modal decomposition of tie-line active power flows*, IEEE Trans. on Power Syst., **32**, 2, pp. 1304–1314 (2017).
16. J. Zhou, W. Zhu, Y. Zheng, C. Li, *Precise equivalent model of small hydro generator cluster and its parameter identification using improved grey wolf optimizer*, IET Gener., Transm. & Distrib., **10**, 9, pp. 2108–2117 (2016).
17. M. K. Transtrum, A. T. Sarić, A. M. Stanković, *Measurement-directed reduction of dynamic models in power systems*, IEEE Trans. on Power Syst., **32**, 3, pp. 2243–2253 (2017).
18. A. M. Azmy, I. Erlich, *Identification of dynamic equivalents for distribution power networks using recurrent ANNs*, IEEE PES Power Systems Conference and Exposition, New York, NY, USA, 2004.
19. J. J. Sanchez-Gasca, J. H. Chow, *Computation of power system low-order models from time domain simulations using a Hankel matrix*, IEEE Trans. on Power Syst., **12**, 4, pp. 1461–1467 (1997).
20. S. A. Y. Sabir, D. C. Lee, *Dynamic load models derived from data acquired during system transients*, IEEE Trans. on Power Appar. and Syst., **PAS-101**, 9, pp. 3365–3372 (1982).
21. J. A. de Kock, F. S. van der Merwe, H. J. Vermeulen, *Induction motor parameter estimation through an output error technique*, IEEE Trans. on Energy Conversion., **9**, 1, pp. 69–76 (1994).
22. O. Benmiloud, S. Arif, *Optimal dynamic equivalence based on multi-objective formulation*, 3rd International Conference on Electrical Sciences and Technologies in Maghreb (CISTEM), Algiers, Algeria, 2018.
23. A. Savio, F. Bignucolo, R. Sgarbossa, P. Mattavelli, A. Cerretti, R. Turri, *A novel measurement-based procedure for load dynamic equivalent identification*, IEEE 1st International Forum on Research and Technologies for Society and Industry Leveraging a better tomorrow (RTSI), Turin, Italy, 2015.
24. O. Benmiloud, S. Arif, *Model order reduction of power systems preserving tie line flows*, International Conference on Applied Smart Systems (ICASS), Medea, Algeria, 2018.
25. J. M. Ramirez, *Obtaining dynamic equivalents through the minimization of a line flows function*, Int. J. of Electrical Power & Energy Syst., **21**, 5, pp. 365–373 (1999).
26. J. H. Chow, G. Rogers, *Power System Toolbox Manual*, Cherry Tree Scientific Software, 2000.
27. P. Kundur, *Power System Stability and Control*, McGraw-Hill, 1994 [chapter 4].
28. T. Tudorache, I. D. Ilina, L. Melcescu, *Parameters estimation of an induction motor using optimization algorithms*, Rev. Roum. Sci. Techn. – Électrotechn. Énerg., **61**, 2, pp. 121–125 (2016).
29. Y. Oubbati, S. Arif, *Transient stability constrained optimal power flow using improved particle swarm optimization approach*, Rev. Roum. Sci. Techn. – Électrotechn. Énerg., **61**, 4, pp. 331–337 (2016).
30. X. S. Yang, *Nature-Inspired Metaheuristic Algorithms*, Luniver Press, Second Edition, 2010.
31. S. Anbarasi, S. Muralidharan, *Intelligent tuning of proportional integral derivative controller using hybrid bacterial foraging particle swarm optimization for automatic voltage regulator system*, Rev. Roum. Sci. Techn. – Électrotechn. Énerg., **62**, 3, pp. 325–331 (2017).
32. M. Younes, *Hybrid method for optimal power flow determination*, Rev. Roum. Sci. Techn. – Électrotechn. et Énerg., **57**, 3, pp. 249–258 (2012).
33. X. S. Yang, S. Deb, *Cuckoo search via Lévy flights*, World Congress on Nature & Biologically Inspired Computing (NaBIC), Coimbatore, India, 2009.
34. X. S. Yang, S. Deb, *Cuckoo search: recent advances and applications*, Neural Computing and Applications, **24**, 1, pp. 169–174 (2014).
35. P. Barthelemy, J. Bertolotti, D. S. Wiersma, *A Lévy flight for light*, Nature, **453**, pp. 495–498 (2008).
36. S. Mirjalili, A. H. Gandomi, S. Z. Mirjalili, S. Saremi, H. Faris, S. M. Mirjalili, *Salp swarm algorithm: A bio-inspired optimizer for engineering design problems*, Advances in Engineering Software, **114**, pp. 163–191 (2017).
37. G. I. Sayed, G. Khoriba, M. H. Haggag, *A novel chaotic salp swarm algorithm for global optimization and feature selection*, Applied Intelligence, **48**, 10, pp. 3462–3481 (2018).
38. S. Mirjalili, *SCA: A Sine Cosine Algorithm for Solving Optimization Problems*, Knowledge-Based Systems, **96**, pp. 120–133 (2016).
39. A. A. Heidari et al., *Harris Hawks Optimization: Algorithm and Applications*, Future Generation Computer Systems, 2019.